

Article

Development of a Novel Hydrodynamic Sequencing Batch Reactor for Landfill Leachate Treatment by Shortcut Biological Nitrogen Removal

Minkyung Kim ¹, Kyung Mo ¹, Moonil Kim ^{1,*} and Fenghao Cui ^{2,*} 

- ¹ Department of Civil and Environmental Engineering, Hanyang University, 55 Hanyangdaehak-ro, Ansan City 426-791, Kyeonggido, Republic of Korea; zsegogok@hanyang.ac.kr (M.K.); nambird@hanyang.ac.kr (K.M.)
- ² Center for Creative Convergence Education, Hanyang University, 55 Hanyangdaehak-ro, Ansan City 426-791, Kyeonggido, Republic of Korea
- * Correspondence: moonilkim@hanyang.ac.kr (M.K.); choibongho7@hanyang.ac.kr (F.C.); Tel.: +82-31-400-4096 (F.C.); Fax: +82-31-502-5142 (M.K.)

Abstract: This study introduced an alternative shortcut biological nitrogen removal (SBNR) process for landfill leachate treatment by developing a novel hydrodynamic sequencing batch reactor (H-SBR). The reactor could enhance the oxygen transfer rate (OTR) and nitrite accumulation ratio (NAR) by modifying internal hydrodynamic turbulence intensity. The average chemical oxygen demand (COD) and total nitrogen (TN) concentrations introduced into the reactor were 660 and 250 mg L⁻¹, respectively, and the average removal efficiencies were 93% (COD) and 96% (TN). The effect of geometric parameters on oxygen transfer was estimated by performing a hydrodynamic model and a nonlinear least square analysis. After correcting the constants (α and β) of mass transfer coefficients ($K_L a$) to values of 0.7361 and 1.2639, the model data fit the experiment well with an R-squared value of 0.99. The OTR improved by up to 30%, and hence, increased the NAR by up to 20% with a reduction of about 0.5 kg N kW⁻¹ for power efficiency. The H-SBR development is innovative because the oxygen transfer efficiency was improved by the hydrodynamic modification of internal turbulence intensity, although not by mechanical equipment or chemical supplements. For the SBNR process, the modification of the reactor configuration for OTR enhancement could significantly improve nitrogen removal efficiency with successful nitrite accumulation. In addition to landfill leachate treatment, the H-SBR process can be employed in the treatment of low C/N ratio wastewaters.

Keywords: nitrogen removal; nitrite accumulation; wastewater treatment; oxygen transfer rate; hydrodynamic model



Citation: Kim, M.; Mo, K.; Kim, M.; Cui, F. Development of a Novel Hydrodynamic Sequencing Batch Reactor for Landfill Leachate Treatment by Shortcut Biological Nitrogen Removal. *Processes* **2023**, *11*, 1868. <https://doi.org/10.3390/pr11071868>

Academic Editors: Krishnamoorthy Rambabu and Kit Wayne Chew

Received: 30 May 2023
Revised: 19 June 2023
Accepted: 20 June 2023
Published: 21 June 2023



Copyright: © 2023 by the authors. Licensee MDPI, Basel, Switzerland. This article is an open access article distributed under the terms and conditions of the Creative Commons Attribution (CC BY) license (<https://creativecommons.org/licenses/by/4.0/>).

1. Introduction

Landfilling results in inevitable leachate percolation from solid wastes; hence, proper treatment of landfill leachate is essential to prevent threats posed to the surroundings by high concentrations of organics, ammonia, and other toxic pollutants [1]. The shortcut biological nitrogen removal (SBNR) process is adopted because it can address the practical problem of treating high-strength wastewater with a low C/N ratio [2,3]. In the SBNR process, ammonia is not completely converted to nitrate but is retained in nitrite to shorten the conventional nitrification-denitrification process [4,5]. This process can theoretically save about 25% of the oxygen supply and 40% of carbon sources [6,7]. Therefore, the SBNR process has significant potential advantages over conventional biological nitrogen removal in terms of reduced energy consumption, carbon source supplementation, and chemical management. The SBNR process has been proposed as a designable technology, particularly to remove high concentration nitrogen from wastewater with a low C/N ratio [3,8].

Partial nitrification, in which nitrogen remains in the ammonia oxidation stage without nitrite conversion to nitrate, is a key step in accomplishing a successful SBNR process. Partial nitrification has to be performed under a strictly controlled low oxygen ($0.5\text{--}2\text{ mg O}_2\text{ L}^{-1}$) environment to achieve reduced oxygen supply and inhibition of nitrite-oxidizing bacterial growth [9,10]. Since oxygen is an essential electron acceptor for aerobic respiration, oxygen availability has a significant influence on the activity of ammonia-oxidizing bacteria (AOB) under limited dissolved oxygen (DO) conditions. It has been determined that the low oxygen transfer rate (OTR) due to the low solubility of oxygen could be a considerable rate-limiting step in partial nitrification [11–13]. Oxygen transfer can be the controlling process for microbial growth. Therefore, it is decisively important to smoothly transfer oxygen from the gas to the liquid phase to limit its consumption by liquid-dwelling microorganisms.

Fine bubble aeration, pure oxygen aeration, and automated oxygen control techniques have been developed as the main alternatives to improve the oxygen transfer rate in biological reactors [14–16]. However, the implementation of these technologies requires mounting specialized equipment and implementing complex modeling support. These obligations may not be flexible to the ever-varying environment of biological treatment reactors. In the field of hydrodynamic studies, it was found that the OTR could be subject to hydrodynamic and physicochemical parameters [17–19]. Studies on the computational fluid dynamics (CFD) model have revealed that the OTR is directly related to the hydrodynamics inside bioreactors [20,21]. In particular, it has been shown that higher turbulence intensity leads to an increase in the oxygen mass transfer coefficient, and hence oxygen uptake [22–24].

Achieving consistent nitrite accumulation in the nitrification process is a vital prerequisite for the development of the SBNR process [25,26]. To obtain nitrite accumulation through selectively washing out nitrite-oxidizing bacteria (NOB), the single reactor system for high activity ammonium removal over nitrite (SHARON) process used short (1–2 days) sludge retention time (SRT) and mesophilic temperatures ($30\text{--}35\text{ }^\circ\text{C}$) [27–29]. In another approach, a high pH (pH 8.0–8.5) or a low DO ($1\text{--}2\text{ mg O}_2/\text{L}$) was used to preferentially slow nitrite oxidation and wash out NOB [29,30]. Nevertheless, the sludge wash-out is not a sensible option in the sequencing batch reactor (SBR) process because it reduces slow-growing denitrifying bacteria and lowers nitrogen removal efficiency [31]. Furthermore, the maintenance of particular STR, temperature, pH, and DO are sensitive and challenging conditions for reactor operation. Therefore, this study proposes a novel SBNR process that enhances OTR with hydrodynamic mechanic configuration. In this process, the sludge wash-out is not essential, and the changes in operating ranges (pH, DO, and temperature) are more acceptable.

The purpose of this study is to perform a novel shortcut nitrogen removal process for the treatment of landfill leachate. A particular configuration of sequencing batch reactor was designed to increase the turbulence intensity inside the bioreactor, which improved OTR and hence nitrogen removal efficiency. A hydrodynamic model of oxygen transfer was developed to investigate the effects of mixing and mass transfer inside the reactors.

2. Materials and Methods

2.1. Reactor Development and Operation

The reactor developed in this study consists of a gas chamber in which gas-liquid phases of air circulation occur in each divided section, enhancing turbulence intensity and oxygen transfer efficiency. Figure 1 shows the configuration of the hydrodynamic sequencing batch reactor (H-SBR). The cylinder structure reactor was made of acrylic glass material with a height of 1.2 m, a diameter of 0.12 m, and an effective volume of 7.5 L. The reactor was divided into 25-cm high sections, and an inlet tube of 4 cm in length and an inner diameter of 1.5 cm was installed in the divided layers of each section. Each divided section creates a gas chamber that circulates air between liquid and gas phases and breaks up large bubbles into smaller bubbles. This setup is designed to increase the intensity of turbulent flow inside the reactor. Seeding sludge was obtained from a biological nitrogen

removal reactor at Ansan wastewater treatment plant, Republic of Korea. The initial mixed liquor-suspended solids (MLSS) concentration in the reactor was 3250 mg L^{-1} . The reactor was operated in sequencing batch mode at a mesophilic temperature of $35 \text{ }^\circ\text{C}$. One cycle of the reactor operation consisted of 0.08 h (hours) of inflow, 32 h of internal anoxic mixing, 20 h of aeration, 14 h of internal anoxic mixing, and 0.25 h of gravity discharge. The hydraulic retention time (HRT) was 2.7 days. Under anoxic conditions, the mixing inside the reactor is carried out by the continuous internal recycling of mixed liquid with a flow rate of 1.5 L h^{-1} . During the aeration stage, the dissolved oxygen (DO) concentration was controlled at $1.5\text{--}2.0 \text{ mg L}^{-1}$ by adjusting the aeration intensity. For comparative studies, an identical configuration of the normal sequencing batch reactor (N-SBR) without section divisions to increase turbulence intensity was operated under identical conditions. The leachate used as influent wastewater was collected from the sanitary landfill of the resource circulation center located in Gapyeong-gun, Republic of Korea. The pH of the landfill leachate ranged between 8.1 and 8.8 (the average pH was about 8.5). The detailed characteristics of landfill leachate are shown in Table 1.

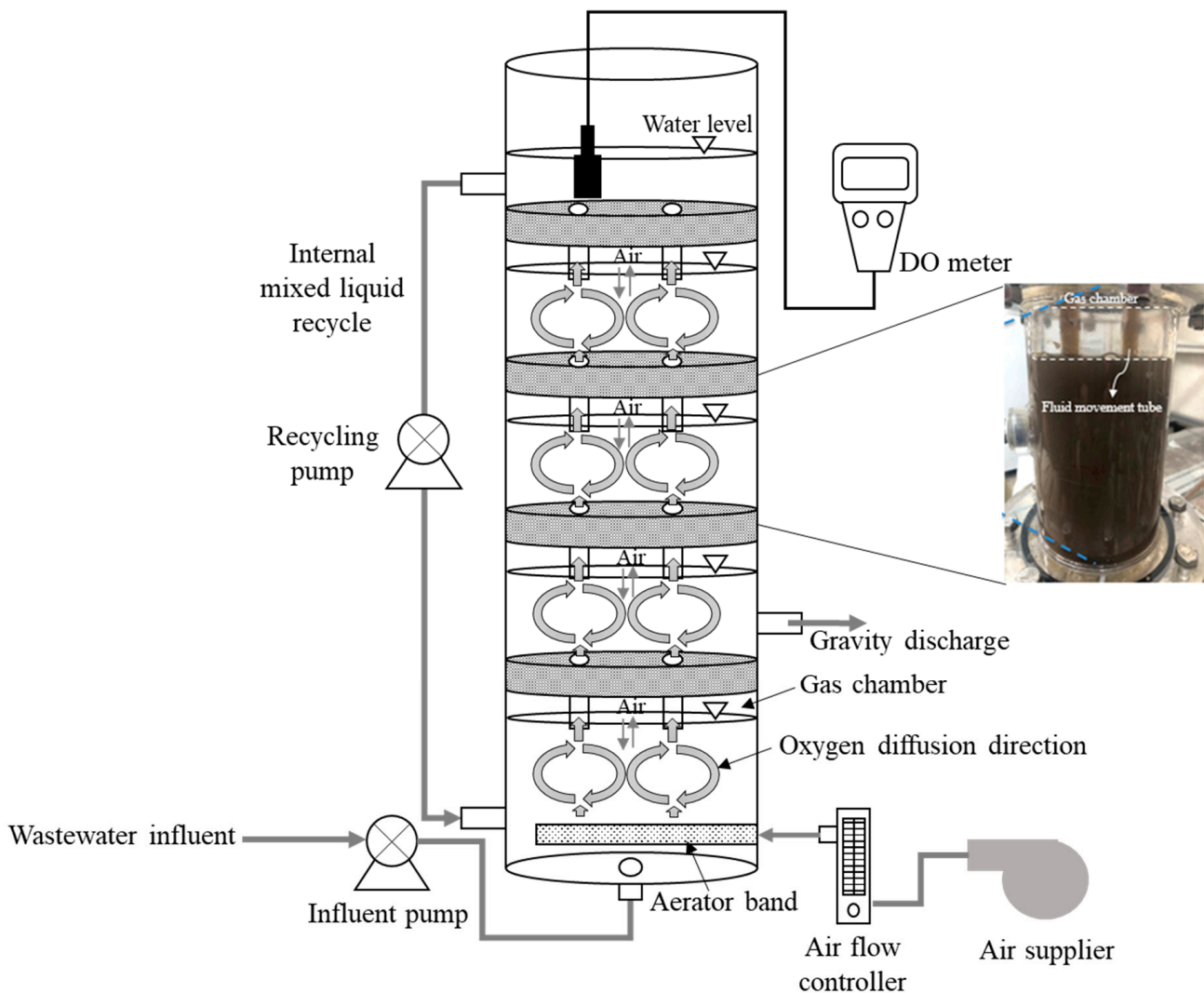


Figure 1. Illustration of H-SBR process.

Table 1. Characteristics of landfill leachate (influent wastewater).

Parameter	Unit	Value (Average ± Standard Deviation)
Total chemical oxygen demand (TCOD)	mg L ⁻¹	1050 ± 230
Soluble chemical oxygen demand (SCOD)	mg L ⁻¹	667 ± 120
Total phosphorous (T-P)	mg P L ⁻¹	25 ± 4
Total nitrogen (T-N)	mg N L ⁻¹	268 ± 23
Ammonia nitrogen (NH ₄ ⁺ -N)	mg N L ⁻¹	93 ± 15
Nitrite nitrogen (NO ₂ -N)	mg N L ⁻¹	140 ± 10
Nitrate nitrogen (NO ₃ -N)	mg N L ⁻¹	41 ± 5.9
Alkalinity	mg CaCO ₃ L ⁻¹	459 ± 24

2.2. Hydrodynamic Mass Transfer Models and Calculating Methods

The non-steady-state modeling method was employed to describe oxygen transfer by values of mass transfer coefficient and OTR (oxygen transfer rate) [17]. Representing the rate of oxygen accumulation equal to the effective rate of oxygen transfer of the OTR at any given instant can be described by the following equation:

$$\frac{dC_t}{dt} = OTR = K_L a \cdot (C_{st} - C_t) \quad (1)$$

where C_{st} is the equilibrium concentration of oxygen in water (mg L⁻¹), C_t is the oxygen concentration in the water at the moment time (mg L⁻¹), and $K_L a$ is the volumetric mass transfer coefficient.

The equilibrium concentration of oxygen in water (C_{st}) is calculated as follows:

$$C_{st} = k \cdot S_{O_2} \cdot \frac{P + h/2}{P} \quad (2)$$

where P is the atmospheric pressure (kPa), h is the aerator band submerged (m), S_{O_2} is the oxygen solubility in pure water at standard atmospheric pressure, and k is the correction factor for the oxygen solubility.

The following expression is written by assuming that the mass transfer coefficient depends on the geometric and dynamic parameters.

$$K_L a = 0.041 \cdot \left(\frac{h}{d}\right)^\alpha \cdot \left(\frac{f}{B}\right)^\beta \cdot \left(\frac{I}{H}\right) \quad (3)$$

where d is the diameter of bubbles (m), f is the aerator band width (m), B is the diameter of the reactor (m), I is the aeration intensity (m³ m⁻² h⁻¹), H is the reactor depth (m), and α and β are the calibrating constants. The calibration of α and β values was performed using the nonlinear least squares method [32,33]. The calculations and modeling graphs were carried out using MATLAB R2021b software (MATLAB R2021b, MathWorks, Portola Valley, CA, USA).

Table 2 shows typical modelling approaches to determine the volumetric mass transfer coefficient.

Table 2. Models for determining volumetric mass transfer coefficient.

Model Type	Equation	Description	Reference
Oxygen transfer model	$K_L a = \frac{1000}{60} \frac{q_c}{C_s}$	Oxygenation capacity q_c refers to the amount of oxygen transferred from the gas phase (bubble) to the unit liquid phase (water) per unit time in an aeration system under standard conditions. Influencing variables for $k_L a$ in cylindrical orbital shaken bioreactors and their corresponding units are the volumetric mass transfer coefficient for oxygen, the reactor diameter (d), the shaking diameter (d_0), the shaking frequency (n), the liquid volume (V_L), the diffusion coefficient for oxygen (DO_2), the kinematic viscosity (ν), and the gravitational acceleration (g).	[13]
Dimensional model	$K_L a = C \left(\frac{n^2 d_0}{g} \right)^\alpha \left(\frac{V_L}{d^3} \right)^\beta \left(\frac{d^3 g}{\nu^2} \right)^\delta \left(\frac{\nu}{DO_2} \right)^\epsilon$	The rate of oxygen transfer in an air-water mixture is assumed to be proportional to the product of the DO deficit, defined as the difference between the saturation concentration and the ambient concentration of dissolved oxygen in water, and the total air-water interfacial area.	[34]
Hydrodynamic model	$K_L a = K_L \frac{\alpha}{1-\alpha} \frac{S_m}{V_m}$		[22]

2.3. Determination of Mass Transfer Coefficient

The OTR was measured under steady-state conditions where the dissolved oxygen concentration remains constant and the oxygen uptake rate (OUR) is equal to the OTR [35]. OUR is calculated by means of an oxygen mass balance around the reactor, and since OUR equals OTR, OTR is quantified as a result. Because the OTR is a function of $K_L a$, the dissolved oxygen concentration at equilibrium conditions (C_{st}), and the oxygen partial pressure in the gas phase (P_{O_2} , kPa), the estimation of the $K_L a$ value with OTR measurement can be expressed by the following calculation.

$$K_L a = \frac{OTR}{C_{st} \cdot P_{O_2}} \quad (4)$$

To determine the mass transfer coefficient at different aeration intensities, the OTR measurements were performed by adjusting the aeration intensities from 2 to 12 $m^3 m^{-2} h^{-1}$ in the reactors (H-SBR and N-SBR).

2.4. Measurement Methods

The real-time monitoring of DO and pH was performed using a DO meter (YSI pro 20, US) and a pH meter (ORION STAR A221, Thermo Scientific Orion, Waltham, MA, USA), respectively. The water samples were filtered using a 1.2 μm filter (GF/C, WHATMAN, Whatman International Ltd., Maidstone, UK) for the analysis of nitrogen compounds. The concentrations of ammonia nitrogen (NH_4-N), nitrite nitrogen (NO_2-N), nitrate nitrogen (NO_3-N), total nitrogen (T-N), and chemical oxygen demand (COD) were measured according to Hach analysis procedures using a spectrophotometer (DR 3900, Hach, Loveland, CO, USA).

The nitrite accumulation ratio (NAR) was calculated by the following equation.

$$\text{NAR} = \frac{\text{NO}_2\text{-N}}{\text{NO}_2\text{-N} + \text{NO}_3\text{-N}} \times 100 \quad (5)$$

3. Results and Discussion

3.1. Performance of SBNR Process

The operations of H-SBR and N-SBR were performed in comparison to investigate differences in SBNR performance. After repeating the one-cycle operation five times or more, stable removals of nitrogen compounds and COD were achieved in both reactors. Figure 2 shows the variations of nitrogen compounds and organics in one-cycle operations of the reactors. The initial concentration of total nitrogen including $\text{NH}_4\text{-N}$, $\text{NO}_2\text{-N}$, and $\text{NO}_3\text{-N}$ in the landfill leachate introduced into the reactor was 250 mg N L^{-1} and the COD concentration was 660 mg L^{-1} , indicating a COD/T-N ratio of 2.64. The $\text{NO}_2\text{-N}$ and COD contained in the leachate were reduced to 10 mg N L^{-1} and 26 mg L^{-1} , respectively, through a denitrification process under the first anoxic conditions. After the first anoxic denitrification process was completed, an aerobic operation for partial nitrification was performed. In the H-SBR, 62 mg N L^{-1} of $\text{NO}_2\text{-N}$ was accumulated at the end of the aerobic operation with the occurrence of nitrite accumulation. However, in the N-SBR reactor, the nitrate concentration was higher than the nitrite concentration. After the aerobic operation, the reactors operated under anoxic conditions again to achieve shortcut nitrogen removal. In this operating period, 400 mg L^{-1} of glucose was supplemented as an external carbon source. $\text{NH}_4\text{-N}$ removal in the N-SBR was incomplete and the effluent nitrogen concentration was higher than in the H-SBR.

Figure 3 shows the average nitrogen (T-N) and organics (COD) removal efficiencies and NAR to compare H-SBR and N-SBR. The T-N removals of H-SBR and N-SBR were 96 and 93%, respectively. The NAR of H-SBR and N-SBR were 60 and 40%, respectively. The NAR of H-SBR was 20% higher than the N-SBR due to improved OTR (see further discussion in the following sections). Both H-SBR and N-SBR showed a similar COD removal efficiency of around 93%. Under identical operating conditions, the H-SBR shows higher nitrogen removal and nitrite accumulation than the N-SBR. The enhancement of the oxygen transfer rate by hydrodynamic modification is estimated to increase nitrate accumulation by up to 20% with an improvement in nitrogen removal efficiency.

During the operation of the SBR cycle, high-strength free ammonia (FA) can be produced due to the influent of high-concentration ammonium with base water. In addition, the partial nitrification process can induce the appearance of free nitrous acid (FNA) with a pH decrease of less than 7. Therefore, the activity of microorganisms can be affected by the simultaneous inhibition of both FA and FNA. The NOB growth rate is more sensitive to FA and FNA changes compared to the AOB. In this study, the AOB growth was abundant, even under high concentrations of FA and FNA. As a result, the AOB can acclimate to changes in the environment, including pH and substrate concentration, and remain effective for ammonia oxidization. On the contrary, the NOB growth was significantly inhibited at a high FA concentration. As a consequence, nitrite oxidization was dramatically restricted in the reactor. In the H-SBR process, the oxygen competition between AOB and NOB could play a complicated role in maintaining the preponderant reaction in the reactor because the slower-growing species can become reduced in number. As obligate aerobes, competition between AOB and NOB for oxygen is critical and it affects the partial nitrification process in ways other than substrate inhibition. Therefore, the OTR enhancement in the H-SBR might create a proper DO affinity environment for the partial-nitrification process.

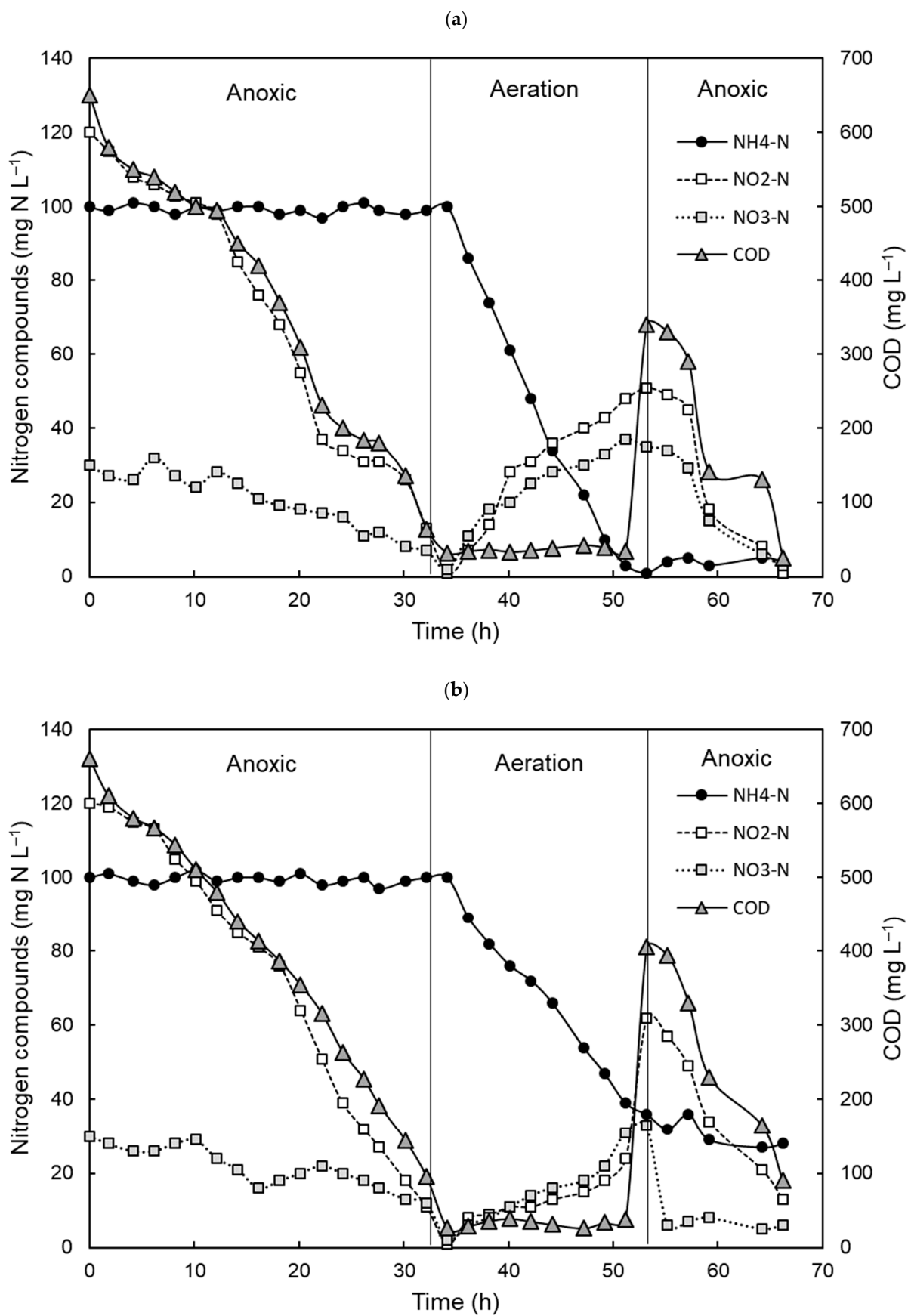


Figure 2. Variations of nitrogen compounds and COD in one-cycle operations of H-SBR (a) and N-SBR (b).

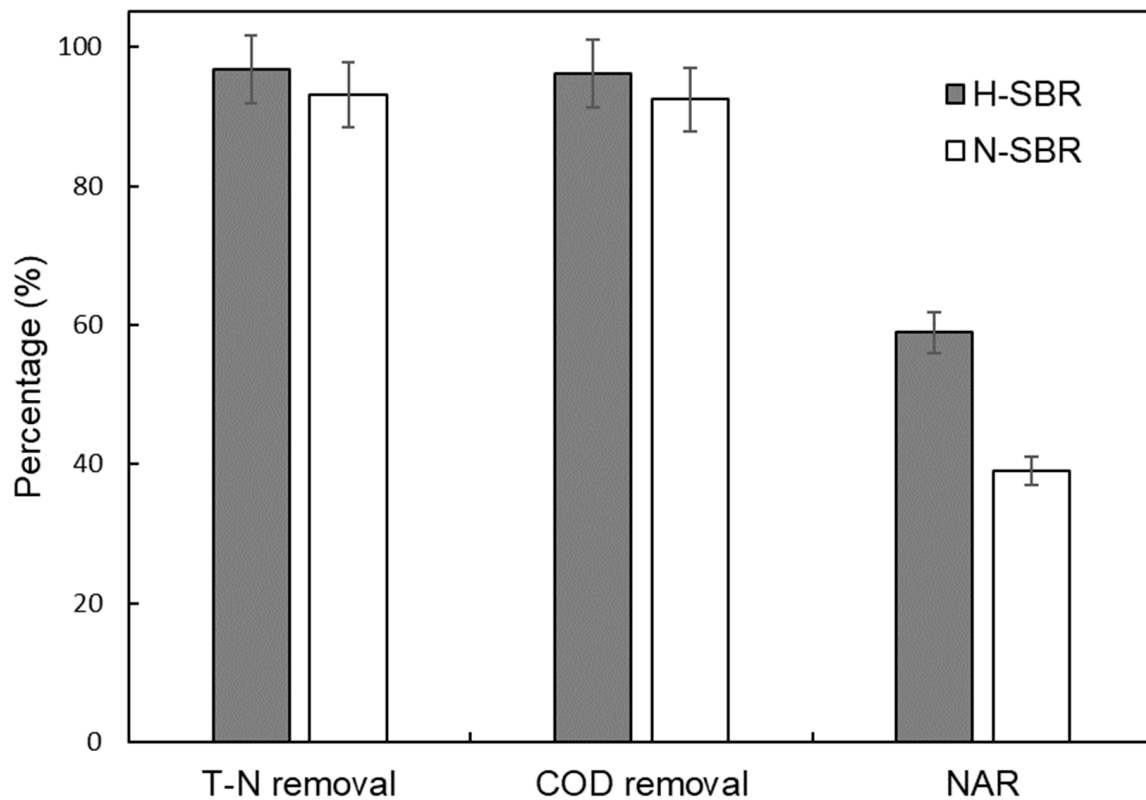


Figure 3. Average organic and nitrogen removal efficiencies and NAR of H-SBR and N-SBR processes (average of three run values).

3.2. Estimation of Mass Transfer Coefficients

The oxygen transfer in the aeration phase has a great influence on the nitrification efficiency because, under low oxygen operation, the oxygen transfer can become an important rate-limiting step. The oxygen mass transfer coefficient depends on certain hydrodynamic and physicochemical factors. This study intended to improve the OTR by increasing turbulence intensity in a modified hydrodynamic aeration reactor. As shown in Figure 4, the constants of Equation (3) were calibrated to estimate the mass transfer coefficient using the geometric and dynamic parameters. The changes in $K_L a$ values were determined at different aeration intensities. Both model outputs of H-SBR and N-SBR showed close proximity to experimental data with R-squared values of 0.99 and 0.96, respectively. The mass transfer coefficient of the H-SBR was 1.5 times higher than that of the N-SBR. This means that the H-SBR can deliver more oxygen to the reactor than the N-SBR under identical reactor geometry and aeration intensity.

3.3. Modeling Hydrodynamic Oxygen Transfer Rate

The hydrodynamic model for the description of oxygen transfer characteristics in the reactor was developed by assuming that the OTR depends on the geometric and dynamic parameters. The key parameters for the model consist of reactor depth, aerator band depth and width, average bubble diameter (determined by the band pore size), aeration intensity, and oxygen solubility. Table 3 shows the parameter values for estimating hydrodynamic OTR changes. Critical differences between H-SBR and N-SBR were the calibrating constants of the mass transfer coefficient equation. The α and β values of H-SBR were 0.7361 and 1.2639, respectively, and for the N-SBR they were 0.6841 and 1.3170, respectively.

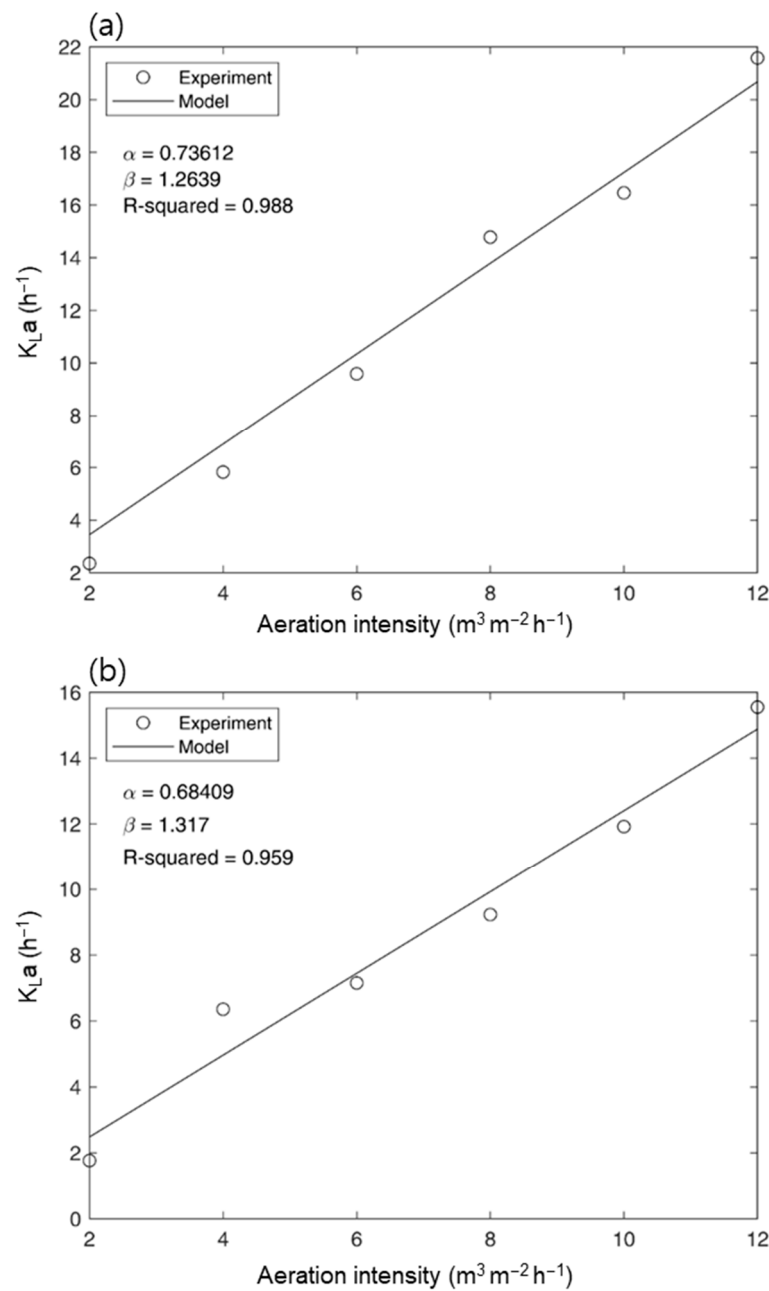
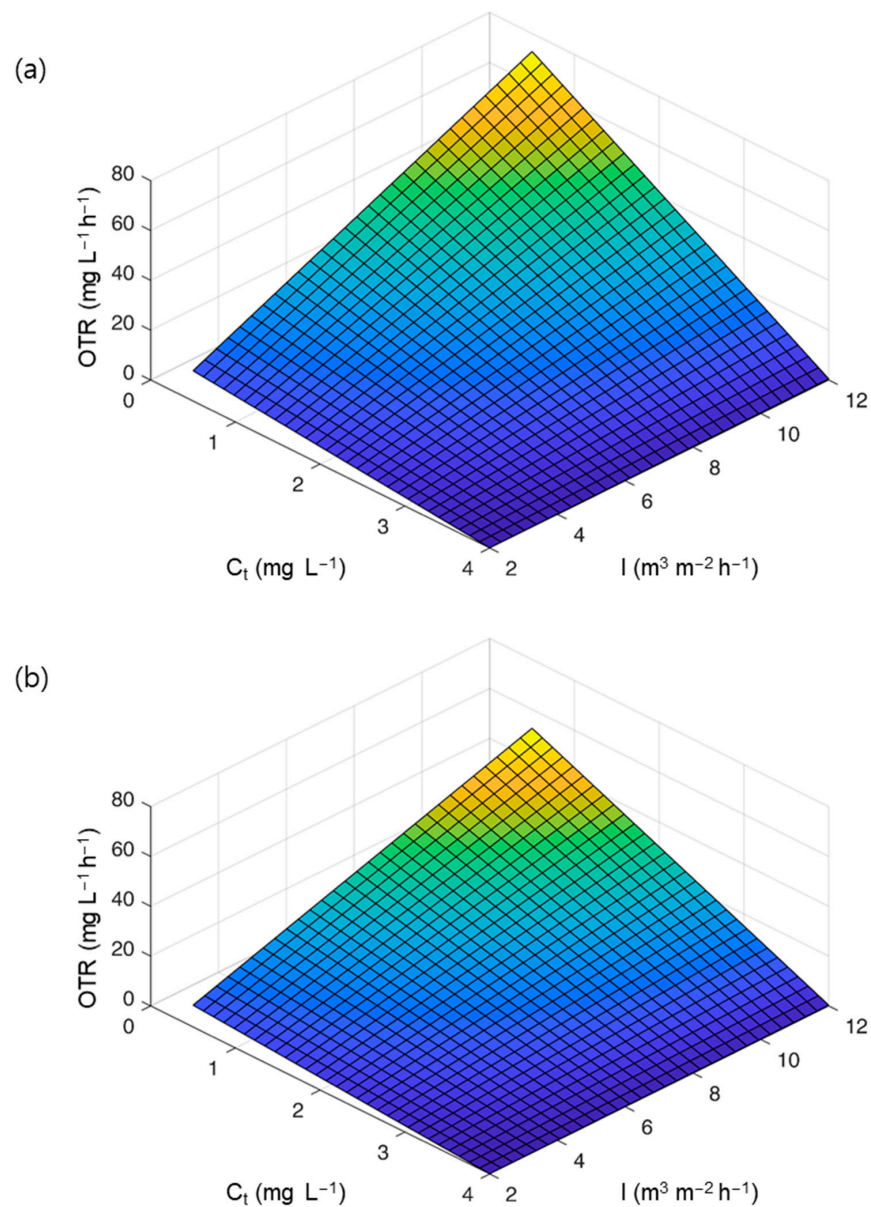


Figure 4. Calibration of mass transfer coefficients using nonlinear least squares regression (a) H-SBR; (b) N-SBR.

Figure 5 shows the changes in OTR at different DO (C_t) levels and aeration intensity (I). At the same aeration intensity, the H-SBR demonstrates higher OTR at lower DO compared to the N-SBR. The OTR tends to enhance with decreasing DO concentration since the rate limiting factor ($C_{st}-C_t$) increases. At $12 m^3 m^{-2} h^{-1}$ of aeration intensity and $0.5 mg L^{-1}$ of DO, the OTR of H-SBR is $63 mg L^{-1} h^{-1}$, which is about 30% higher than the N-SBR ($45 mg L^{-1} h^{-1}$). Operating at low aeration intensity to reduce DO is an important characteristic of the SBNR process because it is directly related to partial nitrification efficiency and energy consumption. The OTR simulation demonstrates that the hydrodynamic enhancement of turbulence intensity can lead to the improvement of OTR, and hence, save on the consumption of power and chemicals.

Table 3. Parameter values for modeling hydrodynamic oxygen transfer rate.

Symbol	Description	Unit	H-SBR	N-SBR
H	The liquid depth in the reactor	m	1.1	1.2
h	The submergence of the aerator	m	1.0	1.1
B	The width of the reactor	m	0.12	0.12
f	The width of the aeration band	m	0.08	0.08
I	The intensity of aeration	$\text{m}^3 \text{m}^{-2} \text{h}^{-1}$	2–12	2–12
d	The average diameter of bubbles	m	0.003	0.003
S_{O_2}	The solubility of oxygen	mg L^{-1}	8.0	8.0
k	The correction factor for oxygen solubility	-		
j	The amount of oxygen in g m^{-3} of air	-	299	299
P	The atmospheric pressure	kPa	101.325	101.325
α	The calibrating constant of the $K_L a$ model	-	0.7361	0.6841
β	The calibrating constant of the $K_L a$ model	-	1.2639	1.3170

**Figure 5.** OTR changes in H-SBR (a) and N-SBR (b) according to DO concentration (C_t) and aeration intensity (I).

3.4. Characteristics of H-SBR Process for Landfill Leachate Treatment

In this study, two types of SBNR reactors with different internal hydrodynamic turbulence were compared. As a result, different characteristics of reactor operating strategies could be established for the treatment of landfill leachate. The N-SBR process, which may represent a conventional shortcut to biological nitrogen removal, withstood a high load with difficulty and required a long aeration time for complete ammonia oxidation. In addition, since the aeration bubbles spiral upward with a short ravel, the fluid contact time reduces, leading to insufficient oxygen utilization. By contrast, in the novel H-SBR process, bubbles remain in the gas retention phase by crushing at each hydrodynamic separation. This study has demonstrated that smaller air bubbles with higher turbulence intensity can create a higher mass transfer coefficient (Figure 4) and higher oxygen transfer efficiency (Figure 5). Therefore, the aeration can be performed at a lower power cost with improved oxygen transfer and utilization efficiencies. Furthermore, this process can withstand a higher load and reduce hydraulic retention time compared to conventional processes. The H-SBR process was estimated to reduce the power efficiency by about 0.5 kg N kW^{-1} .

3.5. Performance Comparisons of SBNR Processes

The SBNR processes for the purpose of landfill leachate treatment and OTR improvement were comparatively studied. The innovative and particular processes for the achievement of shortcut nitrogen removal are a hybrid membrane aerated biofilm reactor (H-MBfR), step-feed partial nitrification simultaneous Anammox and denitrification (SPNAD), up-flow sludge bed/multi-stage oxygen-limited aeration tank/upflow sludge bed (A/O/A), Nano bubble SBR, and SBR. Table 4 shows the comparative performances of different SBNR processes. The shortcut nitrogen removal techniques reduce the amount of aeration required for partial nitrification, thereby reducing the operating load of the air pump to enable economical operation. In addition, depending on influent factors such as reactor configuration, the aeration method, and operating conditions, the criteria for calculating the amount of aeration can affect the OTR, nitrite accumulation, and ammonium removal efficiency. The operation of H-MBfR showed $25.6 \text{ mg L}^{-1} \text{ h}^{-1}$ of OTR and 84% of NAR. By using the Nano bubble generation, the OTR was increased to $36 \text{ mg L}^{-1} \text{ h}^{-1}$ with 60% of NAR. Nevertheless, these techniques were performed by synthetic wastewater applications and have not been demonstrated for industrial wastewater. The application of the SBNR process can be particularly used for the treatment of low C/N ratio wastewater. In landfill leachate treatment case studies, the influent showed a low COD to TN ratio of 1–4. To overcome the shortcoming of insufficient nitrogen removal, conventional techniques employed a system process consisting of aeration and anoxic reactors. Compared to these techniques, the H-SBR process has a technical advantage that carries out simultaneous nitrogen and organic removal in a single-reactor configuration. The H-SBR presented in this study did not show a dramatically different performance compared to other processes in the removal of COD and nitrogen. In the H-SBR operation, partial nitrification can reduce oxygen supply compared to conventional nitrogen removal processes, and further reduce the amount of aeration energy, making it a better alternative considering wastewater treatment efficiency and operating energy cost. For performing a successful SBNR process, consideration of the design process should be given to the selection of the reactor configuration, oxygen transfers and requirement, nutrient balance, and effluent characteristics.

Table 4. Comparisons of operating characteristics and nitrogen removal for different SBNR processes.

SBNR Process	Wastewater	C/N Ratio (COD to TN)	OTR (mg L ⁻¹ h ⁻¹)	NAR (%)	T-N Removal (%)	Reference
H-MBfR	Synthetic wastewater	Partial nitrification	25.6	84	87	[36]
SPNAD	Landfill leachate	1.0	No data	88	98	[37]
A/O/A	Landfill leachate	3–4	No data	68	94	[38]
Nano bubble SBR	Synthetic wastewater	Partial nitrification	36	60	96	[13]
SBR	Landfill leachate	1.3	No data	98	78	[39]
H-SBR	Landfill leachate	2–3	63	60	96	This study

4. Conclusions

This study demonstrated a novel SBNR process that hydrodynamically increases turbulence intensity, and hence, enhances the OTR inside the reactor. The H-SBR operates with landfill leachate of a low C/N ratio with a COD removal of 93% and a nitrogen removal of 96%. Compared to the analogous operation by the N-SBR process, the H-SBR process had a 20% higher NAR, a 30% higher OTR, and a 45% higher power efficiency. The hydrodynamic model estimation has shown that the H-SBR mass transfer coefficient can increase up to 1.5 times compared to that of conventional N-SBR. The improvements in the SBNR performance are innovative because the modification of the internal geometry of the reactor was the only critical adjustment for the OTR and NAR enhancement. In addition to landfill leachate, wastewater treatment with a low C/N ratio, such as anaerobic digester effluent and food industry wastewater, can benefit from the H-SBR application. In this study, the nitrogen removal over nitrite accumulation in a single reactor was significantly improved with the modification of reactor configuration for the hydrodynamic enhancement of OTR.

Author Contributions: F.C. and M.K. (Moonil Kim): conceptualization and project administration; K.M. (Kyung Mo) and M.K. (Minkyung Kim): methodology; F.C. and M.K. (Minkyung Kim): writing original draft; F.C. and M.K. (Moonil Kim): supervision, review, and editing. All authors have read and agreed to the published version of the manuscript.

Funding: This study was supported the Korea Environmental Industry & Technology Institute (KEITI) of the Korea Ministry of Environment (MOE) as part of the “Resource Circulation Policy Response Technology” (2017000710002).

Institutional Review Board Statement: Not applicable.

Informed Consent Statement: Not applicable.

Data Availability Statement: The data that support the findings of this study are available from the corresponding author upon reasonable request.

Conflicts of Interest: The authors declare no conflict of interest.

References

- Kjeldsen, P.; Barlaz, M.A.; Rooker, A.P.; Baun, A.; Ledin, A.; Christensen, T.H. Present and Long-Term Composition of MSW Landfill Leachate: A Review. *Crit. Rev. Environ. Sci. Technol.* **2002**, *32*, 297–336. [\[CrossRef\]](#)
- Zhang, S.J.; Peng, Y.Z.; Wang, S.Y.; Zheng, S.W.; Guo, J. Organic matter and concentrated nitrogen removal by shortcut nitrification and denitrification from mature municipal landfill leachate. *J. Environ. Sci.* **2007**, *19*, 647–651. [\[CrossRef\]](#)
- Huang, X.; Lee, P. Shortcut nitrification/denitrification through limited-oxygen supply with two extreme COD/N-and-ammonia active landfill leachates. *Chem. Eng. J.* **2001**, *404*, 126511. [\[CrossRef\]](#)
- Surmacz-Gorska, J.; Cichon, A.; Miksch, K. Nitrogen removal from wastewater with high ammonia nitrogen concentration via shorter nitrification and denitrification. *Water Sci. Technol.* **1997**, *36*, 73–78. [\[CrossRef\]](#)
- Peng, Y.; Zhu, G. Biological nitrogen removal with nitrification and denitrification via nitrite pathway. *Appl. Microbiol. Biotechnol.* **2006**, *73*, 15–26. [\[CrossRef\]](#) [\[PubMed\]](#)
- Chung, J.W.; Bae, W. Nitrite reduction by a mixed culture under conditions relevant to shortcut biological nitrogen removal. *Biodegradation* **2002**, *13*, 163–170. [\[CrossRef\]](#)

7. Schmidt, I.; Sliemers, O.; Schmid, M.; Bock, E.; Fuerst, J.; Kuenen, J.G.; Jetten, M.S.M.; Strous, M. New concepts of microbial treatment processes for the nitrogen removal in wastewater. *FEMS Microbiol. Rev.* **2003**, *27*, 481–492. [[CrossRef](#)]
8. Cui, F.; Lee, S.; Kim, M. Removal of organics and nutrients from food wastewater using combined thermophilic two-phase anaerobic digestion and shortcut biological nitrogen removal. *Water Res.* **2011**, *45*, 5279–5286. [[CrossRef](#)]
9. Wang, J.L.; Yang, N. Partial nitrification under limited dissolved oxygen conditions. *Process Biochem.* **2004**, *39*, 1223–1229.
10. Cui, B.; Yang, Q.; Liu, X.H.; Huang, S.T.; Yang, Y.B.; Liu, Z.B. The effect of dissolved oxygen concentration on long-term stability of partial nitrification process. *J. Environ. Sci.* **2020**, *90*, 343–351. [[CrossRef](#)] [[PubMed](#)]
11. Baldwin, S.A.; Cheng, T.C.; Demopoulos, G.P. A contribution to the measurement of oxygen mass transfer in a laboratory pressure reactor. *J. Chem. Technol. Biotechnol.* **2000**, *75*, 665–672.
12. Blackburne, R.; Yuan, Z.; Keller, J. Partial nitrification to nitrite using low dissolved oxygen concentration as the main selection factor. *Biodegradation* **2008**, *19*, 303–312. [[CrossRef](#)] [[PubMed](#)]
13. Yao, G.J.; Ren, J.Q.; Zhou, F.; Liu, Y.D.; Li, W. Micro-nano aeration is a promising alternative for achieving high-rate partial nitrification. *Sci. Total Environ.* **2021**, *795*, 148899. [[CrossRef](#)]
14. Suescun, J.; Irizar, I.; Ostolaza, X.; Ayesa, E. Dissolved oxygen control and simultaneous estimation of oxygen uptake rate in activated-sludge plants. *Water Environ. Res.* **1998**, *70*, 316–322.
15. Shammass, N.K.; Wang, L.K. Pure oxygen activated sludge process. In *Handbook of Environmental Engineering*; Wang, L.K., Pereira, N.C., Hung, Y.T., Eds.; Springer: Berlin/Heidelberg, Germany, 2009; Volume 8, pp. 283–314.
16. Duan, Y.; Liu, Y.S.; Zhang, M.M.; Li, Y.Y.; Zhu, W.; Hao, M.Y.; Ma, S.Y. Start-up and operational performance of the partial nitrification process in a sequencing batch reactor (SBR) coupled with a micro-aeration system. *Bioresour. Technol.* **2019**, *296*, 122311. [[CrossRef](#)]
17. Khudenko, B.M.; Shpirt, E. Hydrodynamic parameters of diffused air systems. *Water Res.* **1986**, *20*, 905–915. [[CrossRef](#)]
18. Glover, G.C.; Printemps, C.; Essemiani, K.; Meinhold, J. Modelling of wastewater treatment plants—How far shall we go with sophisticated modelling tools? *Water Sci. Technol.* **2006**, *53*, 79–89. [[CrossRef](#)] [[PubMed](#)]
19. Liotta, F.; Chatellier, P.; Esposito, G.; Fabbicino, M.; Van Hullebusch, E.D.; Lens, P.N.L. Hydrodynamic Mathematical Modelling of Aerobic Plug Flow and Nonideal Flow Reactors: A Critical and Historical Review. *Crit. Rev. Environ. Sci. Technol.* **2014**, *44*, 2642–2673. [[CrossRef](#)]
20. Ertekin, E.; Kavanagh, J.M.; Fletcher, D.F.; McClure, D.D. Validation studies to assist in the development of scale and system independent CFD models for industrial bubble columns. *Chem. Eng. Res. Des.* **2021**, *171*, 1–12. [[CrossRef](#)]
21. Nadal-Rey, G.; McClure, D.D.; Kavanagh, J.M.; Cassells, B.; Cornelissen, S.; Fletcher, D.F.; Germaey, K.V. Computational fluid dynamics modelling of hydrodynamics, mixing and oxygen transfer in industrial bioreactors with Newtonian broths. *Biochem. Eng. J.* **2022**, *177*, 108265. [[CrossRef](#)]
22. Jun, K.S.; Jain, S.C. Oxygen-transfer in bubbly turbulent shear-flow. *J. Hydraul. Eng.* **1993**, *119*, 21–36. [[CrossRef](#)]
23. Herrmann-Heber, R.; Reinecke, S.F.; Hampel, U. Dynamic aeration for improved oxygen mass transfer in the wastewater treatment process. *Chem. Eng. J.* **2020**, *386*, 122068. [[CrossRef](#)]
24. Schwarz, M.; Behnisch, J.; Trippel, J.; Engelhart, M.; Wagner, M. Oxygen transfer in two-stage activated sludge wastewater treatment plants. *Water* **2023**, *13*, 1964. [[CrossRef](#)]
25. Wang, J.W.; Yang, L.X.R.; Zhang, Y.; Zhang, H.P.; Liu, J.J. Partial nitrification characteristics of an immobilized carrier in municipal wastewater under low-temperature shock: The role of the nitrifying bacterial community structure. *Water* **2023**, *15*, 1714. [[CrossRef](#)]
26. Zhang, Z.Z.; Zhang, Y.; Chen, Y.G. Recent advances in partial denitrification in biological nitrogen removal: From enrichment to application. *Bioresour. Technol.* **2020**, *298*, 122444. [[CrossRef](#)]
27. Guo, H.L.; He, T.Y.; Chang, J.S.; Liu, P.; Lee, D.J. Nitrogen removal from low C/N wastewater in a novel Sharon&DSR (denitrifying sulfide removal) reactor. *Bioresour. Technol.* **2022**, *362*, 127789.
28. Shalini, S.S.; Joseph, K. Combined SHARON and ANAMMOX processes for ammoniacal nitrogen stabilisation in landfill bioreactors. *Bioresour. Technol.* **2018**, *250*, 723–732. [[CrossRef](#)]
29. Kosgey, K.; Zungu, P.V.; Bux, F.; Kumari, S. Biological nitrogen removal from low carbon wastewater. *Front. Microbiol.* **2022**, *13*, 968812. [[CrossRef](#)]
30. Magri, A.; Rusalleda, M.; Vila, A.; Akaboci, T.R.V.; Balaguer, M.D.; Llenas, J.M.; Colprim, J. Scaling-up and long-term operation of a full-scale two-stage partial nitritation-anammox system treating landfill leachate. *Processes* **2021**, *9*, 800. [[CrossRef](#)]
31. Bae, W.; Kim, S.; Park, S.; Ryu, H.; Chung, J. Evaluation of predominant factor for shortcut biological nitrogen removal in sequencing batch reactor at ambient temperature. *Bioprocess. Biosyst. Eng.* **2019**, *42*, 1195–1204. [[CrossRef](#)]
32. Scitovski, R. A special nonlinear least-squares problem. *J. Comput. Appl. Math.* **1994**, *53*, 323–331. [[CrossRef](#)]
33. Cui, F.; Park, C.; Kim, M. Application of curve-fitting techniques to develop numerical calibration procedures for a river water quality model. *J. Environ. Manag.* **2019**, *249*, 109375. [[CrossRef](#)]
34. Klockner, W.; Gacem, R.; Anderlei, T.; Raven, N.; Schillberg, S.; Lattermann, C.; Buchs, J. Correlation between mass transfer coefficient $k(L)a$ and relevant operating parameters in cylindrical disposable shaken bioreactors on a bench-to-pilot scale. *J. Biol. Eng.* **2014**, *7*, 28. [[CrossRef](#)] [[PubMed](#)]
35. Clarke, K.G. *An Introductory Engineering and Life Science Approach. Chapter 8—The Oxygen Transfer Rate and Overall Volumetric Oxygen Transfer Coefficient. Bioprocess Engineering*; Elsevier Science: Amsterdam, The Netherlands, 2013; pp. 147–170.

36. Wang, Y.; Zhu, T.; Chang, M.; Jin, D. Performance of a hybrid membrane aerated biofilm reactor (H-MBfR) for shortcut nitrification. *Biochem. Eng. J.* **2021**, *173*, 108089. [[CrossRef](#)]
37. Zhang, F.; Peng, Y.; Wang, S.; Wang, Z.; Jiang, H. Efficient step-feed partial nitrification, simultaneous Anammox and denitrification (SPNAD) equipped with real-time control parameters treating raw mature landfill leachate. *J. Hazard. Mater.* **2019**, *364*, 163–172. [[CrossRef](#)]
38. Wu, L.; Li, Z.; Zhao, C.; Liang, D.; Peng, Y. A novel partial-denitrification strategy for post-anammox to effectively remove nitrogen from landfill leachate. *Sci. Total Environ.* **2018**, *633*, 745–751. [[CrossRef](#)] [[PubMed](#)]
39. Kulikowska, D.; Bernat, K. Nitritation–denitritation in landfill leachate with glycerine as a carbon source. *Bioresour. Technol.* **2013**, *142*, 297–303. [[CrossRef](#)] [[PubMed](#)]

Disclaimer/Publisher’s Note: The statements, opinions and data contained in all publications are solely those of the individual author(s) and contributor(s) and not of MDPI and/or the editor(s). MDPI and/or the editor(s) disclaim responsibility for any injury to people or property resulting from any ideas, methods, instructions or products referred to in the content.